Title
Effect of Electrolyte Composition on the Performance of Sodium/Polymer Cells

Author
Doeff, M.M.

Publication Date
1996-10-01

LBNL-39520
UC-1500
Preprint

ERNEST ORLANDO LAWRENCE
BERKELEY NATIONAL LABORATORY

Effect of Electrolyte Composition on the Performance of Sodium/Polymer Cells

M.M. Doeff, A. Ferry, Y. Ma, L. Ding,
and L.C. De Jonghe
Materials Sciences Division

October 1996
Submitted to
Journal of the Electrochemical Society

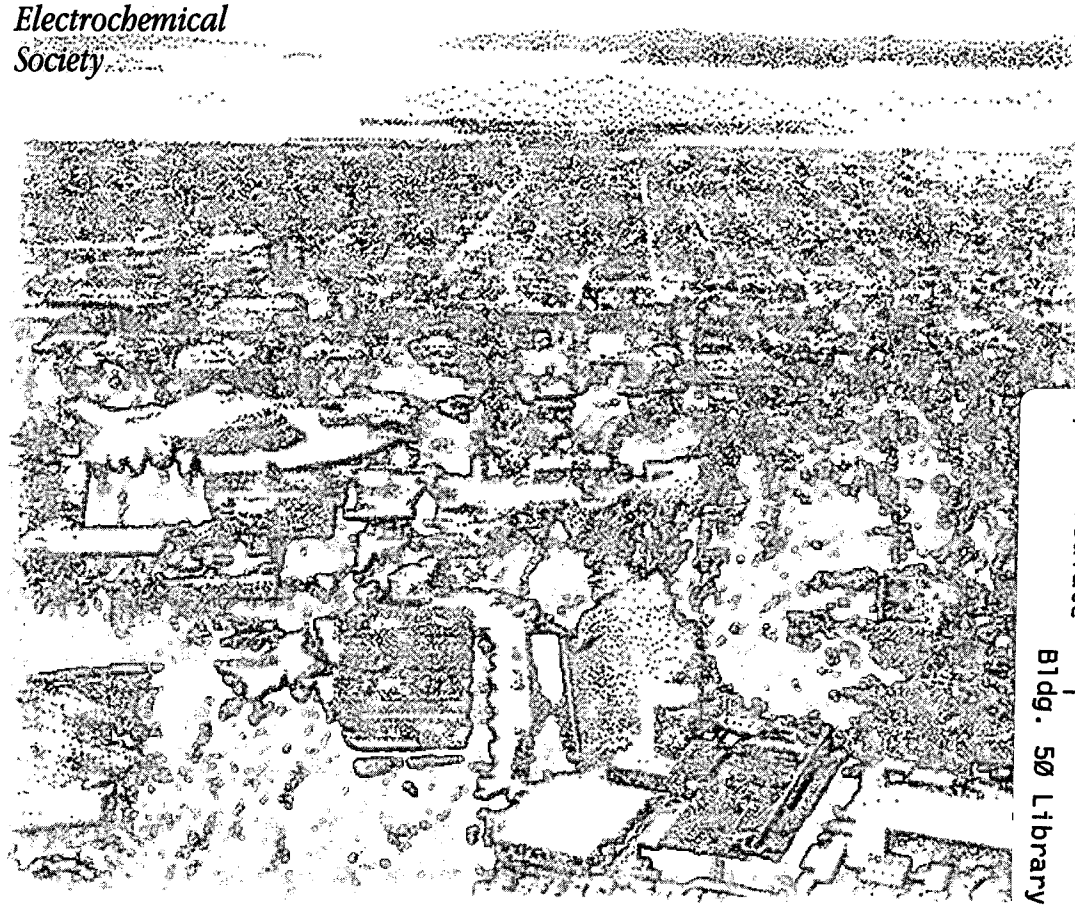

DISCLAIMER

LBNL-39520

Effect of Electrolyte Composition on the Performance of Sodium/Polymer Cells

Marca M. Doeff, Anders Ferry*, Yanping Ma, Lei Ding, and L. C. De Jonghe

Materials Sciences Division
Lawrence Berkeley Laboratory
University of California
Berkeley, CA 94720, U. S. A.

and

* Department of Experimental Physics
Umeå University
Umeå, Sweden 901 87

October, 1996

This work was supported by the Assistant Secretary for Energy Efficiency and Renewable Energy, Office of Transportation Technologies, Office of Advanced Automotive Technologies of the U.S. Department of Energy under Contract No. DE-AC03-76SF00098. A. Ferry would like to thank stiftelsen Blancheflor-Boncompagnie and JC Kempes minnes stipendiefond for financial support.

Effect of Electrolyte Composition on the Performance of Sodium/Polymer Cells

Marca M. Doeff, Anders Ferry*, Yanping Ma, Lei Ding, and L. C. De Jonghe
Materials Sciences Division
Lawrence Berkeley Laboratory
University of California
Berkeley, CA 94720
and
*Department of Experimental Physics
Umeå University
901 87 Umeå, Sweden

Abstract

The dependence of $Na/P(EO)_nNaX/Na_xMnO_2$ (P(EO) = poly(ethylene oxide), X=CF_3SO_3 or $(CF_3SO_2)_2N$)) cell cycle life and rate capability on polymer electrolyte composition is described. Transition time experiments and mathematical modeling indicate that failure due to salt precipitation occurs at $it^{1/2}$= 10.5-21.4 $mAs^{1/2}/cm^2$, when high initial concentrations of $NaCF_3SO_3$ are used in operating cells. Evidence for large ionic clusters in concentrated $PEO/NaCF_3SO_3$ solutions is also seen in the Raman spectroscopic data. Salt precipitation is a direct consequence of the concentration gradients that arise during operation, due to the negative cationic transference numbers (t_+^0) of the binary salt/polymer electrolyte. By decreasing the initial salt concentration, t_+^0 is increased, cell rate capability is doubled and the cycle life is enhanced nearly threefold. Similar improvements are obtained when $PEO/NaN(CF_3SO_2)_2$ electrolytes are used.

Introduction

A recent report described $Na/P(EO)_8NaCF_3SO_3/Na_xMnO_2$ cells[1] that exhibited 100% utilization of the cathode active material at a discharge rate of 0.1 mA/cm^2, although this decreased markedly when the current density was increased. Furthermore, only sixty cycles were obtained before the capacity diminished to less than 50% of theoretical. Corrosion at the sodium/polymer interface[2] and structural changes in the orthorhombic Na_xMnO_2 positive electrode material were ruled out as major causes of capacity fading in these unoptimized devices.[1] The excellent reversibility of Na_xMnO_2 towards electrochemical sodium ion insertion processes was subsequently confirmed by electrochemical potential spectroscopy experiments.[3] Clearly, there were other limitations to performance in these first generation devices.

Significantly, it has recently been shown that the transport properties[4,5] (conductivity, salt diffusion coefficient and cationic transference number, t_+^0) of binary sodium salt/polymer solutions vary considerably with salt type and concentration, and that t_+^0 is low or even negative. Based on these results, it is predicted that premature failure will occur due to the build-up of concentration gradients in the cells during galvanostatic charge or discharge. Depending upon the initial salt concentration and conditions used, this can result in salt depletion or precipitation on one side of the cell, causing incomplete utilization during discharge at high rates.[6]

The present paper describes a study of the effect of electrolyte composition on the rate capability and cycle life of $Na/P(EO)_nNaX/Na_xMnO_2$ cells. The results presented herein indicate that salt concentration and type in the polymer electrolyte can have a

profound effect on performance, and that a thorough understanding of polymer electrolyte transport properties is critical for cell optimization.

Experimental

The cathode active material, orthorhombic Na_xMnO_2, with a nominal composition of x=0.44, was prepared by conventional solid state reactions, or the glycine-nitrate combustion method, as described previously.[7] PEO (Aldrich, average M.W.=5 x 10^6) was used as received. NaTFSI (TFSI=$N(CF_3SO_2)_2$) was prepared from LiTFSI (3M Company) by ion-exchange. The lithium salt was dissolved in acetonitrile, and an excess of $Na_{0.44}MnO_2$ was added (approximately 0.22 Na^+/Mn in $Na_{0.44}MnO_2$ are replaced by lithium ions during 24 hours of equilibration with a stoichiometric amount of lithium salt at room temperature). [7] The solution was stirred for 24 hours and filtered to remove manganese oxide, and the process was repeated. Acetonitrile was removed from the filtrate by rotary evaporation, and the product was dried in air and under vacuum. The white powder was analyzed for Mn, Na, Li, C, N and S content (University of California at Berkeley Micro-analytical Laboratory). Neither manganese nor lithium was detected, and Na, C, N, and S analyses were consistent with a formula of $NaN(CF_3SO_2)_2$. NaTf (Tf=CF_3SO_3) was obtained from Johnson-Matthey (Alfa Products). Prior to use, both salts were stringently dried at elevated temperature under vacuum for several days.

Sodium anodes, composite cathodes, polymer electrolyte separators and cells were prepared as described previously.[8] The capacity per unit area was 0.45 ± 0.11 mAh/cm^2 and the porosity was 0.77±.02 for all composite electrodes. The separator thickness was approximately 70 μm.

Cells, equilibrated for at least one hour at 85°C, were galvanostatically charged and discharged between 1.8 and 3.5 V, using either a computer-controlled EG&G Princeton Applied Research 173 potentiostat/galvanostat or a MacPile II (Biologic SA, Claix, France). Charges were performed at 0.1 mA/cm^2 and discharge rates were varied as described in the text. There was a half hour open circuit period between half-cycles. For the transition time experiments, current densities of 0.55 mA/cm^2 were applied to symmetrical cells. Rest periods of one hour were used between experiments, except where otherwise noted.

FT-Raman spectra with a wavenumber resolution of 1 cm^{-1} were recorded at 85°C using a Bruker IFS 66 equipped with a Raman module FRA 106. During measurements, the sample cell was placed in an evacuated thermostat with a temperature stability of ± 0.3°C.

Results and Discussion

The ionic conductivity (σ), salt diffusion coefficient (D_s), and t_+^0 for several binary salt/P(EO) compositions are listed in Table 1. These examples illustrate the dependence of the electrolyte transport properties upon salt concentration and type.[4,5] For the $P(EO)_nNaTf$ system, both D_s and t_+^0 decrease markedly with increasing salt concentration, and t_+^0 is negative for all but very dilute salt solutions.[4] Negative cationic transference numbers are a consequence of the non-ideality of the salt/polymer solutions, and strongly imply that the ionic current is primarily carried by negatively charged aggregates.

In spite of this, devices containing $P(EO)_nNaTf$ electrolytes still operate successfully, because diffusion of cation-containing species (ion pairs, etc.) due to the induced concentration gradient will occur in a direction opposite to that of cationic migration due to the electric field.[9] According to Doyle et al.[10], however, the concentration gradient, Δc, that develops upon passage of current will become more pronounced as t_+^0 decreases (equation 1).

$$\Delta c \approx \frac{i(1-t_+^0)L}{FD_S} \qquad (1)$$

(i=current density, L=electrolyte thickness , D_S= salt diffusion coefficient).

Depending upon component dimensions, initial salt concentration and current density, either salt precipitation or depletion can occur during operation, resulting in premature failure. Mathematical modeling of a $Na/P(EO)_{12}NaTf/Na$ cell[4,6] undergoing galvanostatic polarization shows that a steeper concentration profile is generated at the anode than the cathode; thus, salt precipitation on the anode side is more likely to occur than depletion on the cathode side. The profile is asymmetrical because of the concentration dependence of the transport properties.

Raman spectroscopy shows that large aggregates of ions are present in concentrated PEO/NaTf electrolyte solutions.[5,11] Figure 1 shows the $\delta_S(CF_3)$ spectral region for crystalline NaTf salt and several PEO/NaTf compositions at 85° C. Components at 747-762 cm^{-1} can, by analogy to the LiTf salt,[12] be assigned to free anions and anions in dissolved aggregates (pairs, triplets, etc.). The feature at 768 cm^{-1} is attributable to anions in larger clusters, possible precursors to salt precipitation, by

analogy to the 1058 cm^{-1} component of the $\nu_S(SO_3)$ mode.[5,11] The Raman data shows that $P(EO)_8NaTf$ solutions contain a significant amount of the clusters, whereas fewer are seen in $P(EO)_{20}NaTf$. The corresponding $\nu_S(SO_3)$ and $\delta_S(CF_3)$ bands of the dry crystalline salt appear at 1059 cm^{-1} and 775 cm^{-1} at 85°C.

Transition time experiments, in which $Na/P(EO)_8NaTf/Na$ cells are galvanostatically polarized, illustrate the phenomenon of salt precipitation (Figure 2). Thick (70 μm) electrolyte membranes and fairly high current densities are used so that semi-infinite diffusion conditions apply $\left(\sqrt{D_s t} << L\right)$. For a fresh cell, polarization occurred after approximately 0.4 hours at 0.55 mA/cm^2, corresponding to a transition time of 21.4 $mAs^{1/2}/cm^2$. This shortened for cells in which current had already been passed, and depended upon the length of the rest and the number of previous polarizations. For a series of consecutive experiments with one hour open circuit periods between applications of current, the transition time converged upon a value of 10.5 $mAs^{1/2}/cm^2$. Note that the initial cell potential upon application of current did not vary significantly over the course of the experiments; thus, these results cannot be explained by increasing interfacial resistance caused, for example, by a reaction between the sodium anode and the polymer electrolyte.

Salt concentrations at the cathode and anode are calculated to be 0.1 M and 12.8 M, respectively, for the pristine cell at the transition time[6] (the starting concentration is 2.58 M for $P(EO)_8NaTf$). The latter value is well above 5.94 M, expected for a possible 3:1 polymer salt crystalline complex similar to those observed in other PEO/sodium salt systems,[13] which perhaps represents the limit of solubility. In fresh cells, the electrolyte

solution may become super-saturated, but in previously operated cells, the presence of nucleation sites allows precipitation to occur sooner (for 10.5 $mAs^{1/2}/cm^2$, the concentration reaches 0.7 M at the cathode and 7.83 M at the anode). The dependence upon the length of the rest reflects the slow kinetics of salt re-dissolution in the polymer.

These results, and the variation of transport properties with salt concentration for the $P(EO)_nNaTf$ system, indicate that better performance at higher current densities should be obtained for an electrolyte composition of $P(EO)_{20}NaTf$ rather than $P(EO)_8NaTf$. Indeed, the transition time experiments strongly suggest that salt precipitation caused the incomplete utilization at higher current densities of the $Na/P(EO)_8NaTf/Na_xMnO_2$ cell in reference 1. To test this theory, cells of identical configuration, but with $P(EO)_{20}NaTf$ electrolytes, were built and cycled.

Figure 3 shows galvanostatic discharges for the $Na/P(EO)_{20}NaTf/Na_xMnO_2$ cell at 85°C. Nearly the full theoretical capacity (approximately 150 mAh/g based on the equivalent weight of $Na_{0.15}MnO_2$) between 3.5 and 1.8 V was obtained during the first discharge at 0.1 mA/cm^2. The curve resembles the open circuit potential profile, which is sloping with several small plateaus.[3] The second and third discharges, at 0.2 and 0.5 mA/cm^2 respectively, were similar to the first, except that the utilization decreased. Capacity fading during the first few cycles is generally not great for this system; thus, Figure 3 shows the rate limitations of the device. Even so, performance was markedly better at higher current densities than for the $Na/P(EO)_8NaTf/Na_xMnO_2$ cell in the earlier report. In fact, the utilization at 0.5 mA/cm^2 of the cell in Figure 1 was approximately equal to that previously obtained at 0.25 mA/cm^2, corresponding to a doubling of the rate capability. The porosities and cathode area capacities for the two cells were nearly

identical; therefore, the improvement is primarily due to the better transport properties of $P(EO)_{20}NaTf$. Furthermore, there is less tendency for precipitation to occur at the anode when lower initial salt concentrations are used, allowing better utilization at higher rates.

For more dilute electrolyte solutions, the possibility of salt depletion during operation should be considered. The rate limitations exhibited by the cell in Figure 3 may, however, have been caused by other factors, such as slow ionic diffusion in the cathode active material.[14] Transition time experiments and mathematical modeling will be useful in predicting when a limiting current is reached in $P(EO)_{20}NaTf$ cells.

Somewhat surprisingly, the change in electrolyte composition also strongly influenced the cycling characteristics of the cell (Figure 4), even at lower rates (0.1-0.2 mA/cm^2). When the $P(EO)_8NaTf$ solution was used, capacity fading was severe; after 27 cycles, there was only 60% utilization, and after 60, less than 50%. For the $P(EO)_{20}NaTf$ example, however, the cycle life was nearly tripled (83 cycles to 60% utilization, and 140 to 50% were obtained). For the $Na/P(EO)_8NaTf/Na_xMnO_2$ cell, diminishing transition times may have caused the observed capacity fading, especially during earlier discharges. Many factors can influence cycling behavior, but it is clear that the poor transport properties of the $P(EO)_8NaTf$ electrolyte predominated in the above example.

P(EO)/NaTFSI electrolytes are more conductive than the P(EO)/NaTf analogs, and cationic transference numbers and salt diffusion coefficients vary less with composition (Table 1).[5] In particular, t_+^0 is less negative at high salt concentrations in the P(EO)/NaTFSI system than it is for P(EO)/NaTf. These results suggest that performance will be less critically dependent upon initial electrolyte composition, although concentration gradients will still develop in operating cells. There is also less likelihood

that precipitation will occur during discharge in cells with concentrated electrolytes, provided that the solubility limit of NaTFSI in PEO is similar to, or greater than, that of other sodium salts, as a recent report has suggested.[15] Thus, compositions may be chosen on the basis of other criteria; e.g., cost, or thermal and mechanical properties, with the caveat that salt depletion is more likely to occur during operation when very dilute solutions are used.

The rate capabilities of cells with $P(EO)_8$NaTFSI, $P(EO)_{10}$NaTFSI and $P(EO)_{20}$NaTFSI electrolytes, indeed, did not vary substantially. They also did not differ much from that of the $P(EO)_{20}$NaTf example. No additional improvement in cycling was seen when $P(EO)_8$NaTFSI or $P(EO)_{10}$NaTFSI electrolytes were used (Figure 4). This indicates that the transport properties of the electrolyte are no longer limiting performance in cells of this configuration, and other factors should be considered for future advances. There is, for example, evidence that irreversible oxidation of the electrolyte, corrosion or other parasitic reactions contributed to the cycling behavior because all of the cells demonstrated slight coulombic inefficiencies during most charges.

The better transport properties of the P(EO)/NaTFSI electrolytes suggest that higher cathode area capacities and loading levels (lower porosities) may be used to increase practical energy density without adversely affecting performance.[16] Transition time experiments, Raman spectroscopy, and mathematical modeling based on knowledge of transport in P(EO)/NaTFSI electrolytes should aid in the design of these improved devices.

Conclusions

It has been shown that performance in Na/P(EO)$_8$NaTf/Na$_x$MnO$_2$ cells was limited primarily by the transport properties of the P(EO)$_8$NaTf electrolyte. Most importantly, mathematical modeling, Raman spectroscopic evidence, and transition time experiments indicated that salt precipitation during operation, especially at higher discharge rates, caused premature failure. This is a direct consequence of the low value of t_+^0 for the highly concentrated electrolyte solution. The rate capability can be doubled and the cycle life approximately tripled by using electrolytes with higher cationic transference numbers; e.g., P(EO)$_{20}$NaTf or P(EO)/NaTFSI solutions. The higher ionic conductivities of the P(EO)/NaTFSI electrolytes suggest that cells with higher practical energy densities than are currently being tested may be used successfully.

Acknowledgment

This work was supported by the Assistant Secretary for Energy Efficiency and Renewable Energy, Office of Transportation Technologies, Office of Advanced Automotive Technologies of the U.S. Department of Energy under Contract No. DE-AC03-76SF00098. A. Ferry would like to thank stiftelsen Blancheflor-Boncompagnie and JC Kempes minnes stipendiefond for financial support.

Table 1. Electrolyte Characteristics

Electrolyte	Electrolyte Characteristics at 85°C		
	σ [S/cm]	D_s [cm^2/s]	t_+^0
$P(EO)_8NaTf$[a]	1.54×10^{-4}	1.47×10^{-8}	-4.37
$P(EO)_{12}NaTf$[a]	1.99×10^{-4}	3.59×10^{-8}	-3.43
$P(EO)_{20}NaTf$[a]	3.13×10^{-4}	4.98×10^{-8}	-0.78
$P(EO)_8NaTFSI$[b*]	6.60×10^{-4}	5.16×10^{-8}	-1.12
$P(EO)_{10}NaTFSI$[b]	6.38×10^{-4}	5.59×10^{-8}	-1.05
$P(EO)_{20}NaTFSI$[b*]	1.09×10^{-3}	5.24×10^{-8}	-0.80

a) From reference 4.

b) From reference 5. (* = interpolated)

References

[1] M. M. Doeff, M. Y. Peng, Y. Ma and L. C. De Jonghe, *J. Electrochem. Soc.*, **141**, L145 (1994).

[2] K. West, B. Zachau-Christiansen, T. Jacobsen, E. Hiort-Lorenzen and S. Skaarup, *Brit. Polymer J.*, **20**, 243 (1988).

[3] M. M. Doeff, L. Ding and L. C. De Jonghe, *Mat. Res. Soc. Symp. Proc.*, **393**, 107 (1995).

[4] Y. Ma, M. Doyle, T. F. Fuller, M. M. Doeff, L.C. De Jonghe and J. Newman, *J. Electrochem. Soc.*, **142**, 1859 (1995).

[5] A. Ferry, M. M. Doeff and L. C. De Jonghe, *Electrochim. Acta*, submitted.

[6] Y. Ma, *Ph.D. Thesis*, University of California at Berkeley, August 1996.

[7] M. M. Doeff, T. J. Richardson and L. Kepley, *J. Electrochem. Soc.*, **143**, 2707 (1996).

[8] Y. Ma, M. M. Doeff, S. J. Visco and L. C. De Jonghe, *J. Electrochem. Soc.*, **140**, 2726 (1993).

[9] G. G. Cameron, J. L Harvie, and M. D. Ingram, *Solid State Ionics*, **34**, 65 (1989).

[10] M. Doyle, T. F. Fuller and J. Newman, *Electrochim. Acta*, **39**, 2073 (1994).

[11] M. Kakihana, S. Schantz, L. M. Torell and J. R. Stevens, *Solid State Ionics*, **40/41**, 641 (1990).

[12] W. Huang, R. Frech and R. A. Wheeler, *J. Phys. Chem.*, **98**, 100 (1994).

[13] a) P. Lightfoot, M. A. Mehta, and P. G. Bruce, *J. Mater. Chem.*, **2**, 379 (1992). b) D. Fauteux, M. D. Lupien and C. D. Robitaille, *J. Electrochem. Soc.*, **134**, 2761 (1987). c) T. Hibma, *Solid State Ionics*, **9&10**, 1101 (1983). d) P. V. Wright, in *Polymer Electrolyte Reviews-1*, (Edited by J. R. MacCallum and C. A. Vincent), p. 61. Elsevier Applied Science, London (1987).

[14] M. M. Doeff, S. J. Visco, Y. Ma, M. Peng, L. Ding and L. C. De Jonghe, *Electrochim. Acta*, **40**, 2205 (1995).

[15] M. Perrier, S. Besner, C. Paquette, A. Vallee, S. Lascaud and J. Prud'homme, *Electrochim. Acta*, **40**, 2123 (1995).

[16] M. Doyle, T. F. Fuller, and J. Newman, *J. Electrochem. Soc.*, **140**, 1526 (1993).

Figure Captions

Figure 1. The CF_3 deformation region of the Raman spectrum for several $P(EO)_nNaTf$ electrolytes and crystalline NaTf at 85° C: $P(EO)_{20}NaTf$ (O), $P(EO)_{12}NaTf$ (▼), $P(EO)_8NaTf$ (◇) and NaTf (●). Components at 747-762 cm^{-1} can be assigned to free anions and anions in dissolved aggregates such as ion-pairs or triplets, and the peak at 768 cm^{-1} is attributable to anions in larger clusters, possible precursors to salt precipitation. The crystalline salt exhibits a narrow band at 775 cm^{-1}.

Figure 2. Transition time experiments for a $Na/P(EO)_8NaTf/Na$ cell at 85°C. The electrolyte thickness was 70 μm. A current density of 0.55 mA/cm^2 was passed across the cell, and a one hour rest period was used between experiments. The number of consecutive polarizations that the cell has undergone is indicated on the graph.

Figure 3. Galvanostatic discharges of a $Na/P(EO)_{20}NaTf/Na_xMnO_2$ cell at 85°C. The first discharge was at 0.1 mA/cm^2, the second at 0.2 mA/cm^2 and the third at 0.5 mA/cm^2. The small spikes in the curves are due to periodic current interrupts lasting a few seconds each.

Figure 4. Discharge capacity as a function of cycle number for Na/Na_xMnO_2 cells with a $P(EO)_8NaTf$ electrolyte at 0.1 mA/cm^2 (from reference 1) (O), a $P(EO)_{20}NaTf$ electrolyte at 0.1 mA/cm^2 (◈) or 0.2 mA/cm^2 (▲), a $P(EO)_8NaTFSI$ electrolyte at 0.1 mA/cm^2 (□) and a $P(EO)_{10}NaTFSI$ electrolyte at 0.1 mA/cm^2 (●).

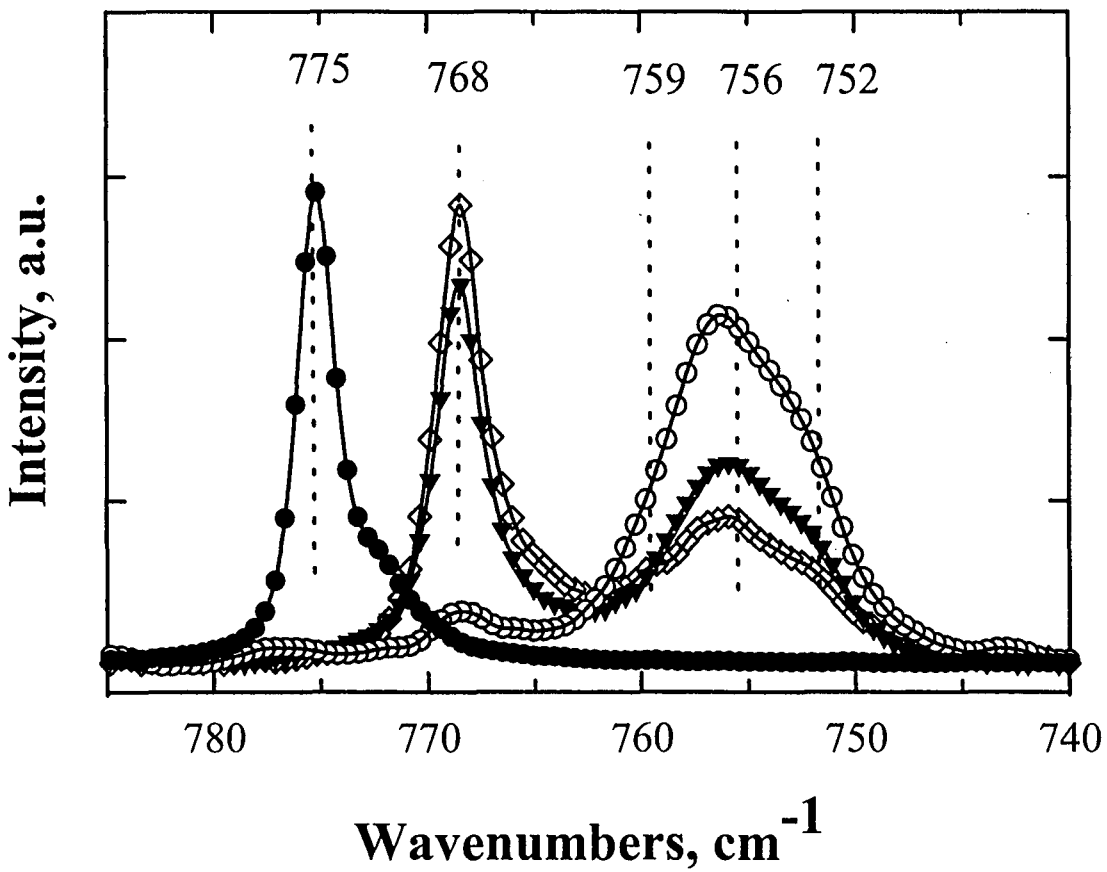

Figure 1 ("Effect of Electrolyte Composition...")

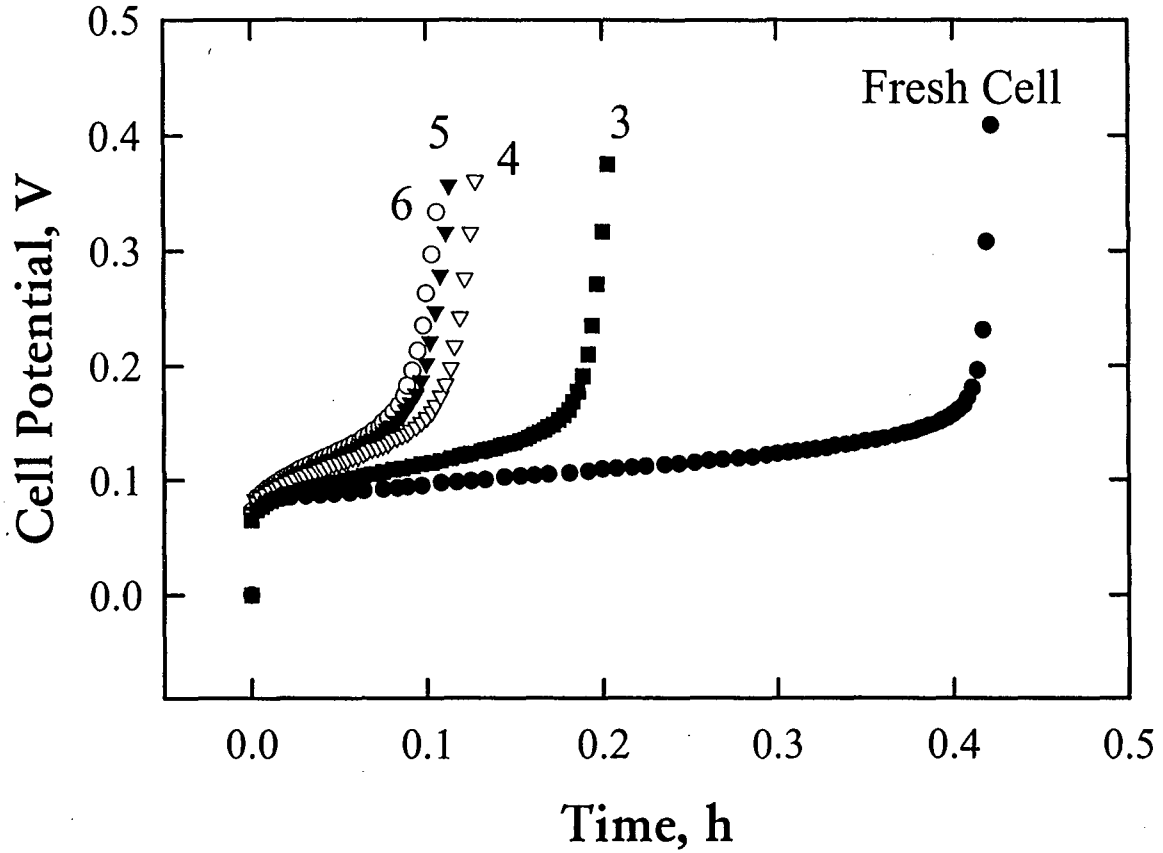

Figure 2 ("Effect of Electrolyte Composition...")

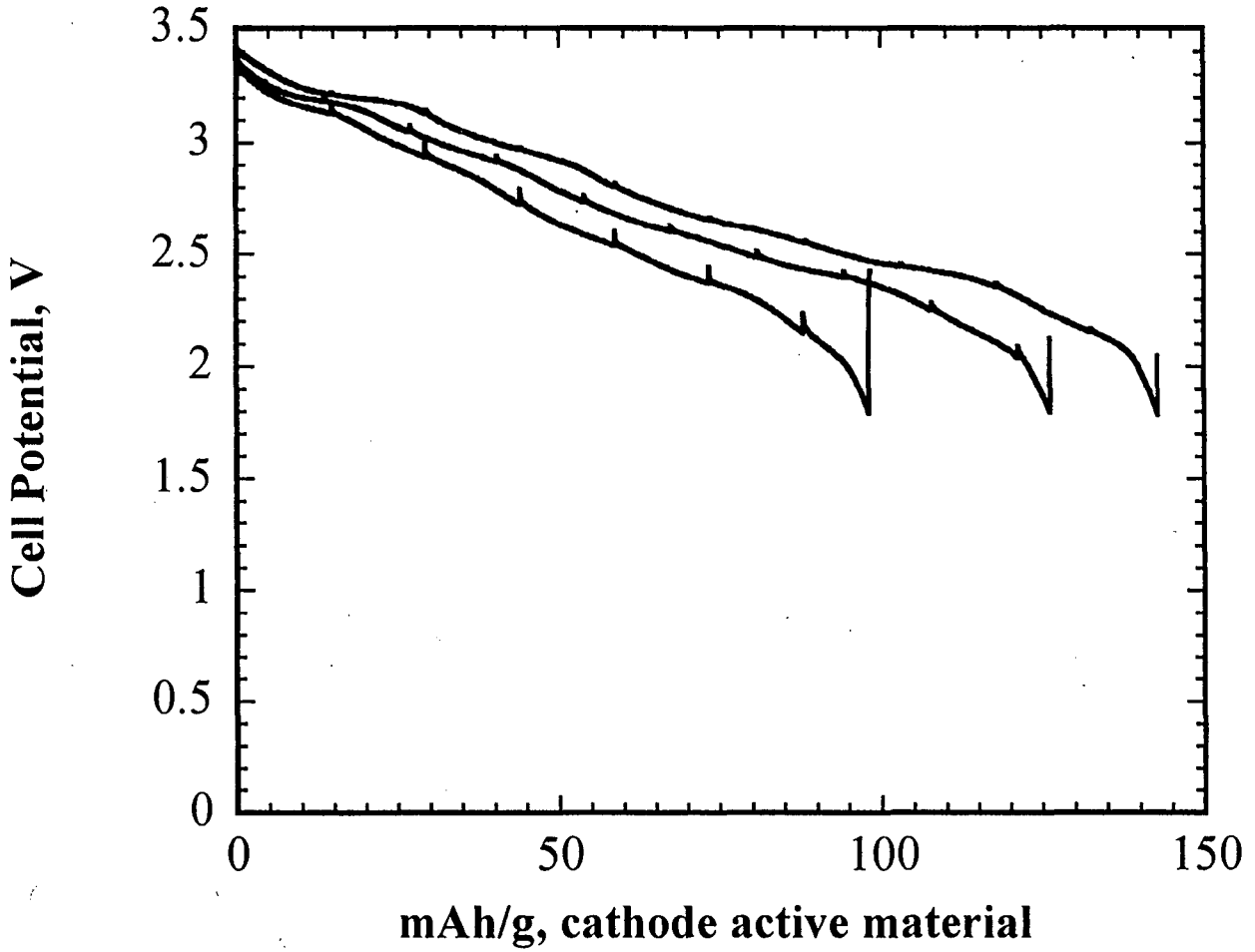
Cell Potential, V
3.5
3
2.5
2
1.5
1
0.5
0
0
50
100
150
mAh/g, cathode active material

Figure 3

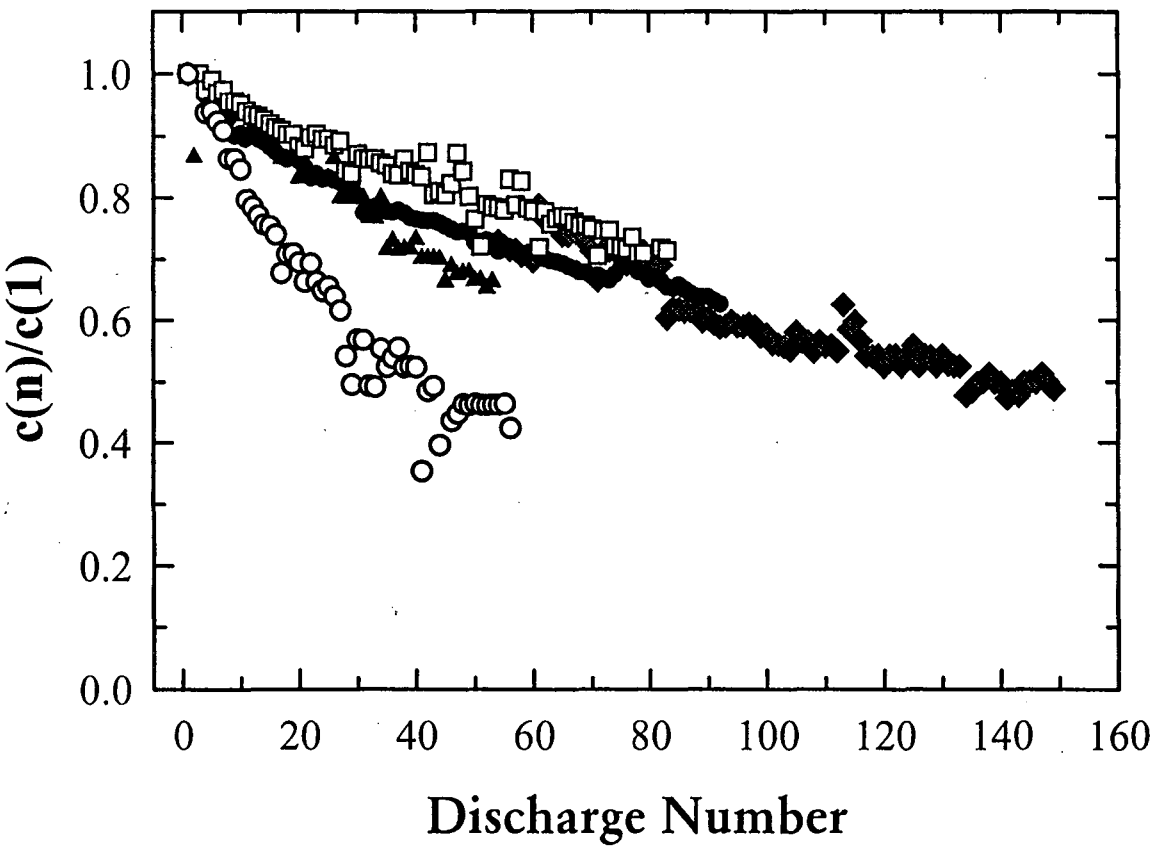

Figure 4
("Effect of Electrolyte Composition"...)

Ernest Orlando Lawrence Berkeley National Laboratory
One Cyclotron Road | Berkeley, California 94720

Prepared for the U.S. Department of Energy under Contract No. DE-AC03-76SF00098